Available online at www.sciencedirect.com
SCIENCE DIRECT
International Journal of Heat and Mass Transfer 49 (2006) 154–158
International Journal of HEAT and MASS TRANSFER
www.elsevier.com/locate/ijhmt

Theoretical analysis on flame dimension in turbulent ceiling fires

W.G. Weng [a,b,*], Y. Hasemi [a]

[a] Department of Architecture, Waseda University, Okubo 3-4-1, Shinjuku-ku, Tokyo 169-8555, Japan
[b] State Key Laboratory of Fire Science, University of Science and Technology of China, Hefei, Anhui 230026, PR China

Received 9 July 2004; received in revised form 17 June 2005
Available online 11 October 2005

Abstract

In this paper, theoretical analysis based on boundary layer theory on flame dimension in turbulent ceiling fires is carried out. The turbulent ceiling fire is developed from a downward round injection source beneath an unconfined inert ceiling. A correlation between the dimensionless flame diameter and the dimensionless heat release rate is obtained, $C_1(S/d) \sim C_2 Q^{*3/4}$. This relation for turbulent ceiling fires is correlated to experimentally measured flame diameters for ceiling fires. Based on the limited data available, the agreement with experiments is very good. Additional experiments are needed to further verify the validity of this relation.
© 2005 Elsevier Ltd. All rights reserved.

Keywords: Ceiling fire; Flame dimension; Boundary layer

1. Introduction

Ceiling fires received scientific attention for the first time in the early seventies [1–3] when scaling laws were developed and correlated to experiments. Orloff conducted experiments using gaseous fuel/inert mixtures flowing through a porous metal burner to simulate the ceiling fires. Observations of their experiments indicated the following flow regimes: laminar, with sheet-like flame; transition, with cell formation; and cellular with a highly convoluted flame. The inception of the cellular flow regime was attributed to a "Rayleigh" instability mechanism. The flame becomes unstable due to gravitational forces acting on the hot diffusion flame burning beneath the cold fuel gases coming from the ceiling located above it. An approximate theory was developed [1–3] to characterize laminar and turbulent (cellular) ceiling fires. The formation of the governing equations and boundary conditions for the laminar regime revealed a 1/5 power dependence on the Grashof number [1]. For the turbulent regime, by making physical arguments and using Spalding's stagnant-film hypothesis [4], a 1/3 power dependence on the Rayleigh number was proposed [2].

Arpaci [5] took a fundamental microscale-based approach to develop scaling laws for laminar and turbulent ceiling fires. A new fundamental dimensionless number characterizing buoyancy driven flames was introduced. A boundary layer thickness and a sublayer thickness for laminar and turbulent ceiling flames, respectively, were proposed in terms of this dimensionless number. A scaling law with power 1/5 and 1/4 were proposed

* Corresponding author. Address: Department of Architecture, Waseda University, Okubo 3-4-1, Shinjuku-ku, Tokyo 169-8555, Japan. Tel.: +81 3 528 63851; fax: +81 3 3209 7214.
E-mail address: wgweng@kurenai.waseda.jp (W.G. Weng).

0017-9310/$ - see front matter © 2005 Elsevier Ltd. All rights reserved.
doi:10.1016/j.ijheatmasstransfer.2005.06.036

Nomenclature

b	Schvab-Zeldovich property in laminar flow, or fluctuating component in turbulent flow
B	transfer number
C_0	constant
C_1, C_2	parameters associated with burner, fuel and ambient air, defined as Eqs. (16) and (17)
C_p	specific heat at constant pressure
d	diameter of burner
D	mass diffusivity
D_β	modified mass diffusivity
g	gravitational acceleration
h	specific enthalpy
H_c	heat release per unit mass of fuel
k	thermal conductivity
l	characteristic length
L_V	heat of vaporization of fuel
$\dot{m}'$	burning rate per unit length at the ceiling
$\dot{m}''$	burning rate per unit area at the ceiling
$\dot{m}'''$	mass generation rate
M_O	molecular weight of oxidizer
p	pressure
$\dot{q}'''$	volumetric heat release rate
Q	heat release per unit mole of fuel
$\dot{Q}$	heat release rate of fuel
Q^*	dimensionless heat release rate
S	flame diameter
T	temperature
u	r-direction velocity
U	r-direction characteristic velocity
v	y-direction velocity
Y_i	mass concentration of species i

Greek symbols

α	thermal diffusivity
β	coefficient of thermal expansion
δ	momentum boundary layer thickness
δ_β	Schvab-Zeldovich property boundary layer thickness
η_β	flame Kolmogorov scale
υ	kinematic viscosity
υ_O	molar stoichiometric coefficient of oxidizer
ρ	density
σ_β	flame Schmidt number

Subscripts

O	oxidizer
W	fuel surface
∞	infinity

for laminar and turbulent ceiling flames, respectively. Comparisons with experimental data [3] showed that the laminar regime correlated well with the proposed theory, and the turbulent regime appeared to correlate with some uncertainty because of the lack of sufficient data.

Flame development under ceiling is very often the direct trigger for the occurrence of flashover during a compartment fire. Experiments have also reported significant change of total flame length after the start of flame development beneath a ceiling in compartment fires [6,7]. As the flames spread in a compartment, it is important to characterize the burning of a surface whose normal is oriented in the direction of gravity, as gravity tends to make the flame undergo transition to cellular flow with a sharp increase in burning rate from an inclined surface to the ceiling configuration [8]. The effect of wind speed and ambient oxygen mass fraction on heat transfer during wind-aided laminar flame spread has also been investigated experimentally in the ceiling configuration [9]. In a recent study, an experimental investigation of the effect of flow velocity, grid-generated turbulence, and buoyancy on the combustion of a solid fuel in a flat plate boundary layer flow in floor and ceiling orientation was conducted [10] and a least square fit to the ceiling data revealed a 1/2 power dependence on the Reynolds number.

In spite of the importance of ceiling fires for fire safety, few works have been conducted on the prediction of the properties of ceiling fires. The studies of Orloff [1–3] and Arpaci [5] only focused on the flame stand-off distance (flame height), and remained the flame diameter equal to the burner diameter. In fact, the flame dimension of a ceiling fire is more important than its flame height since flame spread beneath ceiling is destructive. And so in this paper, theoretical analysis based on boundary layer theory on flame dimension in turbulent ceiling fires is carried out. The theoretical results are compared to Hasemi's experimental data [11–14].

2. Theoretical analysis

Firstly, a brief description of experimental work is introduced in this section for theoretical analysis. In Refs. [11–14], inert unconfined ceiling was produced with two layers of 12-mm thick 1820-mm long square mineral fiber boards, and a steel columnar porous burner was installed at the center of the ceiling with the injection surface downward flush to the ceiling (Fig. 1). No soffit was attached. Two burners of different diameters, 90 mm and 160 mm, were prepared to examine the fuel size effect. The burner was filled with 5-mm

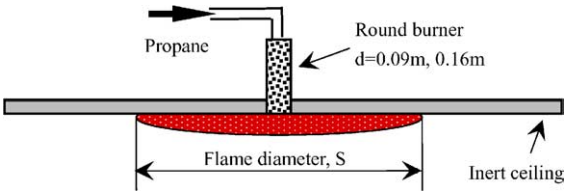

Fig. 1. Experimental setup [11].

diameter ceramic balls and its injection surface was covered by stainless wire mesh. Propane was used as the fuel. Fuel supply rate was monitored with a gas flow meter, and the flame geometry was recorded by digital video. The reported flame diameter is the average over 1 min of the data thus recorded at 1 s interval. The whole apparatus was built beneath a smoke collection hood. Heat release measurement was conducted in the smoke exhaustion duct by the oxygen consumption method. The heat release rate thus measured will be referred to as the effective heat release rate.

While the experiments were conducted by increasing the nominal heat release rate from 5 kW, the flame for 5 kW looked like a cluster of cellular laminar flamelets around the injection source. The present paper deals only with the results at 10 kW and larger, where steadily spreading radial turbulent flame was observed. In addition, the flames with different fuel flow rate are believed to be a same type of turbulent flame due to the ceramic balls in the burners and stainless wire mesh on the injection surface of burners for increasing turbulence.

From the above description, it is clear that the ceiling flames produced from this experimental setup are buoyancy-driven turbulent flames. Though this, first a brief dimensional review of laminar flames is given as necessary background. The steady state laminar diffusion flame equations for the variable-density boundary layer are, briefly [1]:

$$\partial(r\rho u)/\partial r+\partial(r\rho v)/\partial y=0 \tag{1}$$

$$\rho u(\partial u/\partial r)+\rho v(\partial u/\partial y)=(\partial/\partial y)[\rho\upsilon(\partial u/\partial y)]-\partial p/\partial r \tag{2}$$

$$\rho u(\partial h/\partial r)+\rho v(\partial h/\partial y)=(\partial/\partial y)[\rho\alpha(\partial u/\partial y)]+\dot{q}''' \tag{3}$$

$$\rho u(\partial Y_i/\partial r)+\rho v(\partial Y_i/\partial y)=(\partial/\partial y)[\rho D(\partial u/\partial y)]+\dot{m}_i''' \tag{4}$$

where the pressure p is $\partial p/\partial y=\rho g$, g is the gravitational acceleration; the specific enthalpy is $h=\int_{T_\infty}^{T}C_p\,\mathrm{d}T$; and assuming the ideal gas, the state equation is $\rho T=\rho_\infty T_\infty$, where u, v, T, Y_i are the r-direction velocity, the y-direction velocity, the temperature and the mass concentration of species i, respectively. $\dot{q}''', \dot{m}'''$ are the volumetric heat release rate and the mass generation rate. ρ, υ, C_p, α, D are the density, the kinematic viscosity, the specific heat at constant pressure, the thermal diffusivity and the mass diffusivity, respectively.

Consider a dimensional interpretation of the pioneering work of Spadling [4], extended by Arpaci [5,15,16]. Eq. (2) integrated over δ is

$$U\frac{U}{l}\delta+\upsilon\frac{U}{\delta}\sim g\frac{\Delta\rho}{\rho}\delta \tag{5}$$

Here, U and l are the characteristic velocity and length, respectively, and δ is the momentum boundary layer thickness. Also, assuming the Lewis number unity ($D=\alpha$), the balance of the Schvab-Zeldovich (heat + oxidizer) property integrated over δ_β is

$$U\frac{B}{l}\delta_\beta+V_{\mathrm{W}}B\sim D\frac{B}{\delta_\beta} \tag{6}$$

Here, V_{W} is the velocity normal to the fuel surface and δ_β is the Schvab-Zeldovich property boundary layer thickness. The Schvab-Zeldovich variable, b is defined as

$$b=(Y_{\mathrm{O}}Q/\upsilon_{\mathrm{O}}M_{\mathrm{O}}+h)/L_{\mathrm{V}} \tag{7}$$

and the transfer number, B is defined as

$$B=(Y_{\mathrm{O}\infty}Q/\upsilon_{\mathrm{O}}M_{\mathrm{O}}-h_{\mathrm{W}})/L_{\mathrm{V}} \tag{8}$$

where υ_{O} and M_{O} are the molar stoichiometric coefficient and the molecular weight of oxidizer, Q and L_{V} are the heat release per unit mole and the heat of vaporization of fuel, and $h_{\mathrm{W}}=C_p(T_{\mathrm{W}}-T_\infty)$.

Through the equation deduction following Ref. [5], the thermal Kolmogorov scale for buoyancy-driven flows listed below is obtained:

$$\frac{1}{\eta_\beta^4}=\left(\frac{\sigma_\beta}{\sigma_\beta+1}\right)\frac{g}{\upsilon D_\beta}\left(\frac{\dot{m}_{\mathrm{W}}''L_{\mathrm{V}}}{kT_\infty}\right) \tag{9}$$

where η_β is the flame Kolmogorov scale. σ_β is the flame Schmidt number. D_β is the modified mass diffusivity, defined by $D_\beta=(1+B)D$. $\dot{m}_{\mathrm{W}}''$ is the burning rate per unit area in fuel surface. k is the thermal conductivity.

From the local mass balance at the ceiling, the below equation is obtained:

$$\dot{m}_{\mathrm{W}}''=\rho V_{\mathrm{W}}=\rho D\left(\frac{\partial B}{\partial y}\right)_{\mathrm{W}}\sim\rho D\frac{B}{\eta_\beta} \tag{10}$$

By integrating the local mass flux of the fuel at the ceiling over a length l ($l\geqslant d$), d is the diameter of burner, one can write:

$$\dot{m}_{\mathrm{W}}'=\dot{m}_{\mathrm{W}}''d\sim\rho D\frac{B}{\eta_\beta}l \tag{11}$$

where $\dot{m}_{\mathrm{W}}'$ is the burning rate per unit length at the ceiling.

Substituting Eq. (9) and $D=\alpha=\frac{k}{\rho C_p}$ in Eq. (11), the following equation is obtained:

$$\dot{m}_{\mathrm{W}}''d\sim\frac{k}{C_p}Bl\left(\frac{\sigma_\beta}{\sigma_\beta+1}\right)^{1/4}\left(\frac{g}{\upsilon D_\beta}\right)^{1/4}\left(\frac{\dot{m}_{\mathrm{W}}''L_{\mathrm{V}}}{kT_\infty}\right)^{1/4} \tag{12}$$

and so

$$\dot{m}_{\mathrm{W}}''^{3/4}\sim\frac{l}{d}\frac{k}{C_p}B\left(\frac{\sigma_\beta}{\sigma_\beta+1}\right)^{1/4}\left(\frac{g}{\upsilon D_\beta}\right)^{1/4}\left(\frac{L_{\mathrm{V}}}{kT_\infty}\right)^{1/4} \tag{13}$$

$\dot{m}''_{\mathrm{W}} H_{\mathrm{c}} \frac{1}{4}\pi d^2 = \dot{Q}$, and introduce a dimensionless heat release rate:

$$Q^* = \frac{\dot{Q}}{\rho_\infty C_{p\infty} T_\infty g^{1/2} d^{5/2}} \tag{14}$$

where H_{c} and $\dot{Q}$ are the heat release per unit mass and the heat release rate of fuel, respectively. And then the below equation is obtained:

$$C_1(l/d) \sim C_2 Q^{*3/4} \tag{15}$$

where C_1 and C_2 are parameters associated with burner, fuel and ambient air, defined as

$$C_1 = B\left(\frac{\sigma_\beta}{\sigma_\beta + 1}\right)^{1/4} \tag{16}$$

$$C_2 = \left(\frac{4\rho_\infty C_{p\infty} T_\infty g^{1/2} d^{1/2}}{\pi H_{\mathrm{c}}}\right)^{3/4} \frac{C_p}{k}\left(\frac{\upsilon D_\beta}{g}\right)^{1/4}\left(\frac{kT_\infty}{L_{\mathrm{V}}}\right)^{1/4} \tag{17}$$

Next, the scale consideration developed in this section is utilized to correlate experimental data on ceiling fires.

3. Results and discussion

The experimental data are summarized in Table 1. The reported nominal heat release rates were calculated from fuel gas supply rate assuming complete combustion. Flame behavior in these conditions is believed to be dominated by the inertial force far more strongly than the case studied by Orloff [1]. The flame sheet developed steadily beneath the ceiling, and apparently there was no systematic change of flame thickness in the radial direction between $r = 0$ and $r = 0.5S$. Here S is the flame diameter of ceiling fire. Although the color of the flame became thinner with increasing radial distance for approximately $r > 0.5S$, there was no such significant oscillation of the flame itself as normally seen in vertical flames. Simple visualization with artificial smoke suggests the existence of vertical air flow towards the ceiling beneath the flame sheet. From this observation, significant horizontal flow along the ceiling is believed to exist only within the flame. This discontinuity of the flow pattern is probably because of the discontinuity of temperature that makes this ceiling flame a shear-free flow. It is also noteworthy that the effective heat release rate was significantly smaller than the nominal one as seen in Table 1. These suggest significant decrease of the combustion efficiency in a concurrent flame spread beneath a downward horizontal surface. The following analysis will use effective heat release rate as it is believed to affect more directly the flame behavior.

Based on the theoretical analysis using boundary layer theory in the above section, and by assuming that the characteristic length, l is equal to the flame diameter of ceiling fire S, Eq. (15) can be written as

$$C_1(S/d) = C_0 C_2 Q^{*3/4} \tag{18}$$

Fig. 2 shows the variation of the dimensionless flame diameter $C_1(S/d)$ with the dimensionless heat release rate $C_2Q^{*3/4}$. The squares correspond to the experimental data of $d = 0.09$ m, and the triangles correspond to those of $d = 0.16$ m. The ambient temperature and initial temperature of fuel were both set as 300 K, and the temperature of fuel surface was assumed to be 333 K [5]. Various parameters used for Eq. (18) are listed in Table 2. The best least square fit of experimental

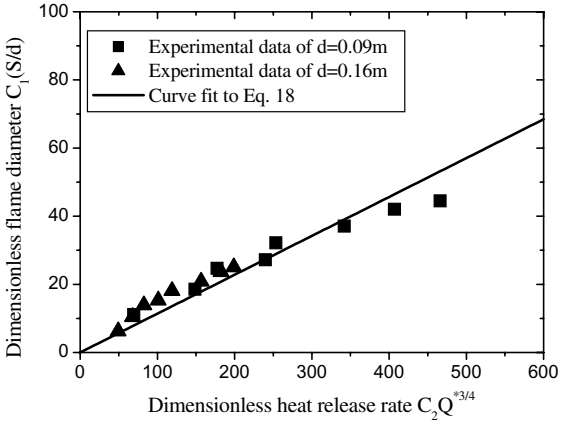

Fig. 2. Variation of the dimensionless flame diameter $C_1(S/d)$ with the dimensionless heat release rate $C_2Q^{*3/4}$.

Table 1
Summary of experimental data [11]

Burner diameter = 0.09 m								
Nominal heat release rate (kW)	10	20	30	40	50	60	70	80
Effective heat release rate (kW)	3.0	8.3	10.5	15.7	16.9	25.2	31.8	38.1
Flame diameter (m)	0.45	0.75	1.00	1.10	1.30	1.50	1.70	1.80
Burner diameter = 0.16 m								
Nominal heat release rate (kW)	10	20	30	40	50	60	70	80
Effective heat release rate (kW)	6.0	9.2	12	15.7	19.5	28.1	34.5	38.7
Flame diameter (m)	0.50	0.70	0.90	1.10	1.30	1.50	1.66	1.74

Table 2
Specified parameters for Eq. (18)

Fuel parameters	
$C_p = 1.6757 \times 10^3$ J/kg K	Specific heat at constant pressure
$g = 9.8$ m/s^2	Gravitational acceleration
$H_c = 50.04 \times 10^3$ J/kg	Heat release per unit mass of fuel
$k = 0.0182$ J/ms K	Thermal conductivity
$L_V = 427.56 \times 10^3$ J/kg	Heat of vaporization of fuel
$M_O = 64 \times 10^{-3}$ kg/mol	Molecular weight of oxidizer
$Q = 2.2 \times 10^6$ J/mol	Heat release per unit mole of fuel
$T_0 = 300$ K	Temperature
$\mu = 8.11$ kg/ms	Dynamical viscosity
$\upsilon_O = 5$	Molar stoichiometric coefficient of oxidizer
$\rho = 1.1817$ kg/m^3	Density
Ambient parameters	
$C_{p\infty} = 1.0057 \times 10^3$ J/kg K	Specific heat at constant pressure
$T_\infty = 300$ K	Temperature
$\rho_\infty = 1.1774$ kg/m^3	Density
Fuel surface parameter	
$T_W = 333$ K	Temperature

data to Eq. (18) gave C_0 as 0.1141. With this constant, close agreement between theory and experiment is seen from Fig. 2. Owing to the sparseness of experimental data in higher $C_2Q^{*3/4}$, this numerical value may be best be considered tentative. New data are needed for more reliable value of this coefficient.

4. Conclusions

Based on boundary layer theory, theoretical analysis on the flame dimension in ceiling fires was carried out. This study proposes a power law (3/4) of the dimensionless heat release rate for the dimensionless flame diameter, $C_1(S/d) \sim C_2Q^{*3/4}$. This relation for turbulent ceiling fires is correlated to experimentally measured flame diameters for ceiling fires. The best least square fit of experimental data to the theory equation gave a constant, with which, close agreement between theory and experiment is seen. Additional experiments are needed to further verify the validity of this relation.

Acknowledgements

The authors would like to acknowledge the supports provided by the Japan Society for the Promotion Science Postdoctoral Fellowship (Grant no. 03246) and the National Natural Science Foundation of China (Grant no. 50306024).

References

[1] L. Orloff, J. De Ris, Modeling of ceiling fires, in: Thirteenth Symposium (International) on Combustion, The Combustion Institute, Pittsburgh, 1971, pp. 979–992.
[2] L. Orloff, J. De Ris, Cellular and turbulent ceiling fires, Combust. Flame 18 (1972) 389–401.
[3] L. Orloff, J. De Ris, Modeling of ceiling flames, Factory Mutual Research Corporation Technical Report 19720, 1970.
[4] D.B. Spalding, The combustion of liquid fuels, in: Fourth Symposium (International) on Combustion, Williams & Wilkins, Baltimore, 1953, pp. 847–864.
[5] V.S. Arpaci, A. Agarwal, Scaling law of turbulent ceiling fires, Combust. Flame 116 (1999) 84–93.
[6] V. Babrauskas, Flame length under ceilings, Fire Mater. 4 (1980) 119–126.
[7] T. Suzuki, A. Sekizawa, H. Satoh, et al. An experimental study of ejected flames of a high-rise building effects of depth of balcony on ejected flames, Proceedings of the Fourth Asia-Oceania Symposium on Fire Science and Technology, Tokyo, Japan, 2000, pp. 363–374.
[8] J. De Ris, L. Orloff, The role of buoyancy direction and radiation in turbulent diffusion flames on surfaces, in: Fifteenth Symposium (International) on Combustion, The Combustion Institute, Pittsburgh, 1974, pp. 175–182.
[9] A. Atreya, K. Mekki, Heat transfer during wind-aided flame spread on a ceiling mounted sample, in: Twenty-fourth Symposium (International) on Combustion, The Combustion Institute, Pittsburgh, 1992, pp. 1677–1684.
[10] L. Zhou, A.C. Fernandez-Pello, Solid fuel combustion in a forced, turbulent, flat plate flow: the effect of buoyancy, in: Twenty-fourth Symposium (International) on Combustion, The Combustion Institute, Pittsburgh, 1992, pp. 1721–1728.
[11] Y. Hasemi, D. Nam, M. Yoshida, Experimental flame correlations and dimensional relations in turbulent ceiling fires, Proceedings of the Fifth Asia-Oceania Symposium on Fire Science and Technology, Newcastle, Australia, Paper 25, 2001, pp. 1–11.
[12] Y. Hasemi, M. Yoshida, R. Takaike, Flame length and flame heat transfer correlations in ceiling fires, Fifteenth Meeting of the UJNR Panel on Fire Research and Safety, National Institute of Standards and Technology, Gaithersburg, vol. 2, 2000, pp. 483–488.
[13] Y. Hasemi, M. Yoshida, Y. Yokobayashi, T. Wakamatsu, Flame heat transfer and concurrent flame spread in a ceiling fire, Proceedings of the Fifth International Symposium on Fire Safety Science, Melbourne, Australia, 1997, pp. 379–390.
[14] Y. Hasemi, M. Yoshita, Flame size and heat transfer correlations for the surface burning of a ceiling and implications for the structure of ceiling flames, J. Archit. Plann. Environ. Eng. 550 (2001) 1–6 (in Japanese).
[15] V.S. Arpaci, A. Selamet, Microscales of buoyancy driven turbulent diffusion fames, Combust. Flame 86 (1991) 203–215.
[16] V.S. Arpaci, Microscales of turbulence and heat transfer correlations, Int. J. Heat Mass Transfer 29 (1986) 1071–1078.